Desalination and Water Treatment
www.deswater.com

28 (2011) 1–7
April

1944-3994/1944-3986 © 2011 Desalination Publications. All rights reserved
doi: 10/5004/dwt.2011.2191

Flux decline and membrane fouling in cross-flow microfiltration of oil-in-water emulsions

Mohsen Abbasi[a], Mohammad Reza Sebzari[a], Abdolhamid Salahi[a], Saeid Abbasi[b], Toraj Mohammadi[a,*]

[a]*Research Centre for Membrane Separation Processes (RCMSP), Faculty of Chemical Engineering, Iran University of Science and Technology (IUST), Narmak, Tehran, Iran*
Tel. +98 21 77240496; email: torajmohammadi@iust.ac.ir
[b]*College of Petroleum and Chemical Engineering, Shiraz University, Mollasadra Street, Shiraz, Iran*

Received 1 March 2009; Accepted 1 July 2010

ABSTRACT

One of the major problems in pressure driven membrane processes is the reduction of the flux to far below the theoretical capacity of the membrane. The typical variation of the flux with time is that of initial rapid decrease followed by a long and gradual decline. The results of an experimental study regarding fouling mechanisms of membrane in separation of oil from oil-in-water emulsions are presented. Mullite microfiltration membranes were synthesized from kaolin clay as MF ceramic membranes. Hermia's models were used to investigate the fouling mechanisms of membranes. The effect of pressure, cross-flow velocity (CFV), temperature and oil concentration on flux decline has been investigated. The results show that cake filtration model can well predict the flux decline of mullite ceramic membranes. After cake filtration model, the best flux predicted to the experimental data was intermediate pore blocking model and worst predicted flux was for complete pore blocking model.

Keywords: Membrane fouling; Microfiltration; Ceramic membranes; Hermia's models

1. Introduction

A large volume of wastewater in the form of either oil-in-water (o/w) or water-in-oil (w/o) emulsions is generated from various process industries such as metallurgical, transportation, food processing and petrochemical as well as petroleum refineries. Typical composition ranges of 'Produced water' generated in the oily wastewater oil and gas industrial processes include 50–1000 mg/l of total oil and grease and 50–350 mg/l of total suspended solids (TSS) [1]. Environmental regulations require that maximum total oil and grease concentration in discharge waters to be 10–15 mg/l [2]. Major pollutant in wastewater (also known as produced water) generating from oil field is oil which may range between 100 and 1000 mg/l or more depending on demulsification efficiency and crude oil nature [3–7]. Removing oil from oil-in-water (oily water) is an important aspect of pollution control. Ceramic membranes have been known for years and used in many different applications depending on their numerous advantages: stability at high temperatures and pressure resistance, good chemical stability, high mechanical resistance, long life and good antifouling properties [8,9]. In these membranes, mullite ceramic membranes have very high chemical and thermal stability and are very cheap because they can be prepared by extruding and calcining kaolin clay.

One of the major inhibiting factors for successful commercialization of the membrane processes is fouling. During membrane filtration, some constituents

*Corresponding author.

Presented at the 1st International Conference on Water and Wastewater Treatment, April 21–22, 2010, Isfahan, Iran

of feed deposits on the membrane surface and/or in the membrane matrix. This retention process is often referred to fouling and results in decrease of the decline flux, eventually leading to membrane replacement. In the last two decades there have been a large number of studies focused on effects of operating parameters on flux decline and membrane fouling mechanisms. In these studies, membrane filtration tests under different experimental conditions were preformed to obtain data on permeates flux variation with time. Although some advances in fundamental MF membrane fouling mechanisms have been achieved, further researches are needed to better understand the fouling mechanisms.

In this work, Hermia's models [10] for dead end filtration were used to investigate the fouling mechanisms involved in cross-flow MF of oil-in-water emulsions. The fitted results of the Hermia's models for cross-flow filtration were presented and compared with the experimental data. Also, more detailed study of the Hermia's models was provided for cross-flow filtration to explain the fouling mechanisms in MF of the oily wastewater.

2. Materials and methods

2.1. Membrane preparation

In this research, mullite MF membranes were synthesized from kaolin clay. The kaolin material used obtained from the Zenooz mine in Marand, Iran. Cylindrical shaped (tubular) membranes (i.d.: 10 mm, o.d.: 14 mm and *L*: 30 cm) were conveniently made by extruding a mixture of about 62–69% kaolin clay and 28–31% distilled water using an extruder. The cylindrical shaped membrane were then dried at room temperature within 48 h and temperature programmed calcinated at 1250 °C for 3 h, suitable calcination period and temperature at which the clay converts to mullite and free silica [11]. Free silica was removed from the calcined membrane by leaching with strong alkali solutions. Removal of this free silica causes microporous tubular ceramic membrane to be made with very high porosity. Free silica removal was carried out with aqueous solutions containing 20% by weight NaOH at a temperature of 80 °C for 5 h. Membranes were washed with distillated water for 12 h at a temperature of 80 °C in order to remove NaOH. Porosity of the membrane before leaching by water absorption method is 32% while after treatment it increases to 48%. PF of the membrane before and after free silica removal at pressure (1 bar), temperature (25 °C) and flow rate (1 m/s) for distillated water are 18 and 35 (l/m^2 h), respectively. Fig. 1 shows the surface and cross-section of the synthetic mullite ceramic membrane.

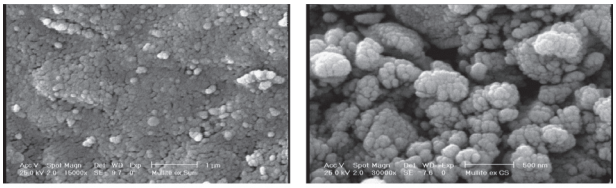

Fig. 1. SEM micrographs of the mullite membrane: (A: surface) and (B: cross-section).

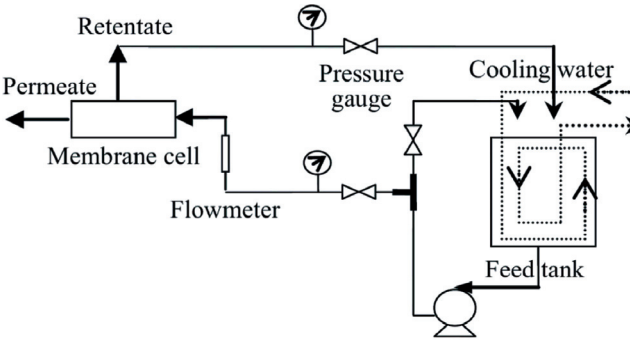

Fig. 2. Microfiltration setup.

2.2. Setup

In order to carry out the experiments almost close to an industrial scale, a pilot plant was designed. The pilot was operated in cross-flow mode. The membrane surface area in contact with the feed was equal to 110 cm^2. The MF cell was installed in a system according to Fig. 2 and all the industrial reservations were considered during the experiments.

The system was simple and had no complexity, however, it was designed in such a way that all important operating parameters in the MF process such as temperature, operating pressure and linear flow velocity could be tuned and controlled. The system mentioned above had a vessel with a capacity of 10l. This vessel had a heater to heat the feed or to keep it at a constant temperature and also a stirrer in order to keep the feed uniform. The feed temperature was controlled by a digital thermometer with an accuracy of ± 0.1 °C. A tubular heat exchanger was used to control the feed temperature.

2.3. Process feed

Synthetic oily wastewaters (oil-in-water emulsions) were prepared by various mixing of condensate gas (C_8–C_{12}) and distillated water with an addition of approximately 0.01 wt.% Triton X–100 emulsifier to the mixture for stabilized emulsion. Condensate gas from Seraje, Ghom, Iran, was used for preparation of the oil–water emulsions. A blender mixed mixture at high shear rate (6000 rpm) for 30 min. Under these conditions,

mean diameter of emulsion is 1.07 μm and emulsions had high stability for employing in MF experiments.

3. Modeling

In the present work, an approach followed by Hermia was used for the description of filtration phenomenon in cross-flow MF of the oily wastewater. In the preceding section, description of the assumptions made and the conclusions reached by the usual and theoretical models for the flux decline is presented. Hermia models are the most useful and applicable models for microfiltration flux decline prediction. The general equation is as follows [12]:

$$\frac{dj}{dt} = -K_j(J - J_0)J^{2-n} \tag{1}$$

where n = 2.0 for 'complete' blocking; n = 1.5 for standard blocking; n = 1.0 for incomplete pore blocking (intermediate fouling) and n = 0 for cake filtration (see Fig. 3). K_j is a constant and J_0 is the limiting flux.

3.1. Cake formation model

Cake/gel formation usually occurs when particles/oil droplets larger than the average pore size accumulate on the membrane surface, forming a "cake/gel". As time goes on, the cake/gel grows and provides an additional porous barrier through which the liquid must permeate. As a result, the cake/gel may increase the particles/oil droplets removal efficiency of the membrane; however, it also increases the membrane resistance and subsequently diminishes flux. For the cake filtration model it is assumed that: (a) Shear stress is proportional to shear rate (Newtonian). (b) All the particles/oil droplets are dimensionally similar, solute deposits on the membrane surface by superimposition forming a compressible cake/gel of uniform thickness. (c) The resistance offered by the cake/gel is directly proportional to the volume filtered. (d) All the particles/oil droplets are retained on the membrane surface and the flux decline phenomenon is solely dependent upon the cake/gel formation (i.e., no sealing of pores). As a result, it can be described as follows:

$$\frac{1}{J^2} = \frac{1}{J_0^2} + K_g t \tag{2}$$

where J_0 and K_g are the initial permeate flux and the constant of the cake/gel formation model, respectively [12,13].

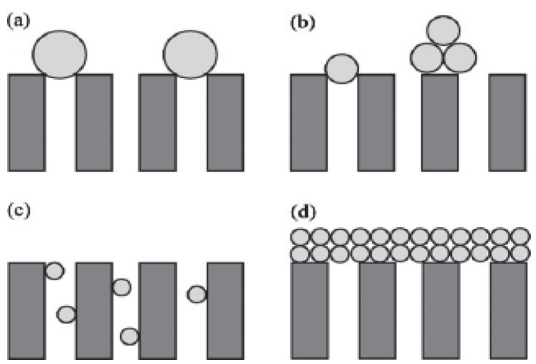

Fig. 3. Schematic representation of blocking mechanism: (a) complete pore blocking, (b) intermediate blocking, (c) standard blocking, (d) cake layer formation.

3.2. Standard pore blocking model

Standard pore block is the most dominant phenomenon when retained particles/oil droplets are dimensionally smaller than the average pore size of the membrane. It is often called adsorptive fouling or pore narrowing. In this case, particles/oil droplets in the fluid approach the membrane, enter into the pores, and adhere to the inner pore walls. Unlike the complete pore plugging model, there is no complete blocking of pores. In this case, the adhesion of particles/oil droplets to the walls decreases the available pore diameter and increases the membrane resistance. Over a period of time the pore diameter decreases and it leads to complete pore blocking. For developing the model, it is assumed that the fluid is Newtonian, and only pore narrowing takes place and not complete pore blocking. Permeate flux can be obtained by the following equation:

$$\frac{1}{J^{1/2}} = \frac{1}{J_0^{1/2}} + K_S t \tag{3}$$

where K_s is the constant in standard pore blocking [12,13].

3.3. Complete pore blocking model

It typically occurs when the particles/oil droplets are dimensionally similar to the mean pore size of the membrane. In this model, particles/oil droplets plug individual pores. As individual pores are plugged, the flow is diverted to other pores that plug successively. Eventually, this reduces the available membrane area and increases the membrane resistance. Due to this fact, the membrane loses its filtration performance and requires cleaning or replacement. The assumptions made for developing this model are:

(a) Every particle participates in the plugging process by sealing one pore on, and once a pore is blocked, other particles/oil droplets do not enter that pore and superimpose on that particle/oil droplet (i.e., no gradual pore blocking).
(b) There is no cake formation.
(c) Feed is Newtonian.

Permeate flux can be simply represented by the following equation:

$$Ln(J) = Ln(J_0) - K_C t \quad (4)$$

where K_C is the constant in complete pore blocking model [12,13].

3.4. Intermediate pore blocking model

This model assumes each particle/oil droplet can block some membrane pores or settle on other particles/oil droplets previously blocked some other pores with superposition of particles/oil droplets. Permeate flux can be obtained by the following equation:

$$\frac{1}{J} = \frac{1}{J_0} + K_i A t \quad (5)$$

where K_i is the constant in intermediate pore blocking model and A is membrane surface [12,13].

4. Results and discussion

4.1. Predicted permeation flux by pore blocking models

Firstly, the relationship between time (t) and permeate flux (J) was drawn for all the TMPs levels. In all cases, the permeate volume decreased with time. In order to ensure precise analysis of the filtration mechanism and also to avoid unsteady state conditions, the permeate data during first 30 s of filtration process was neglected. The models that were defined by Hermia for the description of various filtration laws were applied to permeate flux data that were obtained in the current studies. A linear relationship of $1/J^2$ versus t, $1/J^{0.5}$ versus t, Ln(J) versus t and $1/J$ versus t was determined experimentally for cake filtration model, standard pore blocking model, complete pore blocking model and intermediate pore blocking model to calculate constants (K) in models. As represented in Figs. 4–7 the filtration data at different TMP levels were compared by prediction flux of cake filtration model, standard pore blocking, complete pore blocking and intermediated pore blocking model.

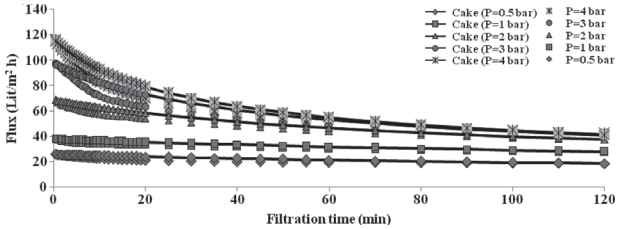

Fig. 4. Permeate flux predicted by the cake layer formation model at different pressure with time (flow rate 1 m/s, oil concentration 1000 ppm and temperature 25 °C).

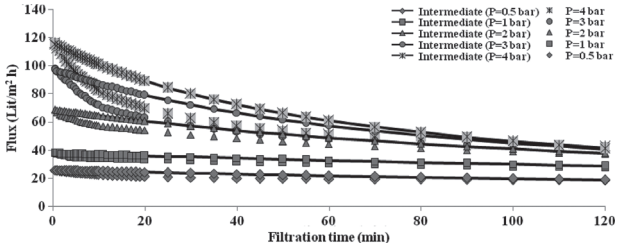

Fig. 5. Permeate flux predicted by the intermediate pore blocking model at different pressure with time (flow rate 1 m/s, oil concentration 1000 ppm and temperature 25 °C).

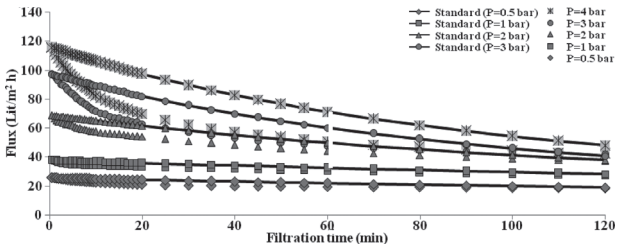

Fig. 6. Permeate flux predicted by the standard pore blocking model at different pressure with time (flow rate 1 m/s, oil concentration 1000 ppm and temperature 25 °C)

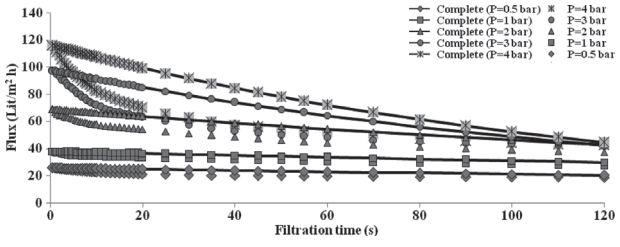

Fig. 7. Permeate flux predicted by the complete pore blocking model at different pressure with time (flow rate 1 m/s, oil concentration 1000 ppm and temperature 25 °C).

To determine whether the data agreed with any one of the models considered, deviation of each plot for one model was compared with the other two. Compared to all the plots for the models, the cake filtration model showed better prediction with relative to the standard pore blocking and intermediate pore blocking models. Results show that average percentage error of predicated flux for cake layer formation model, intermediate pore blocking model, standard pore blocking model and complete pore blocking model is 7.64%, 11.83%, 14.75% and 16.70%, respectively. High deviations between experimental and predicted flux decline were observed for the complete pore blocking model. It must be noted that oil droplets are deformable. Therefore, cake density, resistance and compression and the rate of flux decline are expected to increase with pressure.

Figs. 8–11 show the fitting of the experimental permeates flux mullite membranes to the pore blocking models for all the experimental conditions tested to indicate effect of CFV on flux decline. Results show that cake filtration model and intermediate pore blocking model have better prediction to standard pore blocking model. The intermediate blocking fouling mechanism occurs when the membrane pore size is similar to the size of particles/oil droplets [12]. Membrane pores are blocked near their entrance in the feed side. Therefore, the intermediate blocking model provided a better agreement to the experimental data than the complete blocking model and standard blocking model, as expected. The average percentage error of predicated flux for cake layer formation model, intermediate, standard and complete pore blocking model is 9.32%, 17.49%, 22.42% and 28.33%, respectively.

Figs. 12–15 represent effect of feed temperature on fouling mechanisms. Results show that cake filtration model and intermediate pore blocking model have better prediction to standard pore blocking model. The standard blocking mechanism occurs when the size of the particles/oil droplets is lower than that of membrane pores. An internal pore blocking is produced due to the adsorption of particles/oil droplets onto the membrane pore walls. As a result, the standard pore blocking model only predicts accurately permeate flux decline with time when variations in permeate flux with time are big [14].

Results illustrate that the fitting of the standard blocking mechanism to the experimental results is not good for mullite ceramic membrane. It must be noted that the highest deviations between experimental and predicted flux decline were observed for the same experimental conditions as in the case of the complete blocking model. The average percentage error of predicated

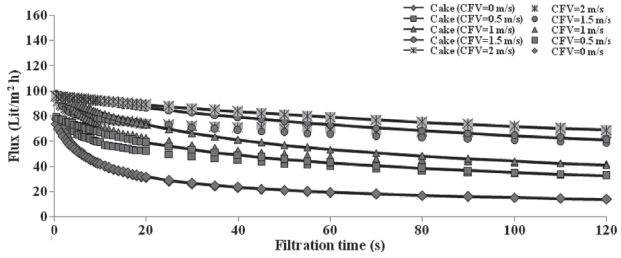

Fig. 8. Permeate flux predicted by the cake layer formation model at different cross flow velocity with time (pressure 3 bar, oil concentration 1000 ppm and temperature 25 °C).

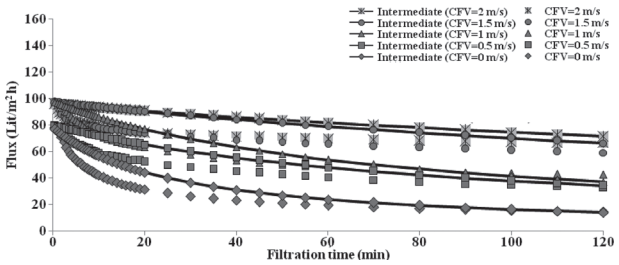

Fig. 9. Permeate flux predicted by the intermediate pore blocking model at different cross flow velocity with time (pressure 3 bar, oil concentration 1000 ppm and temperature 25 °C).

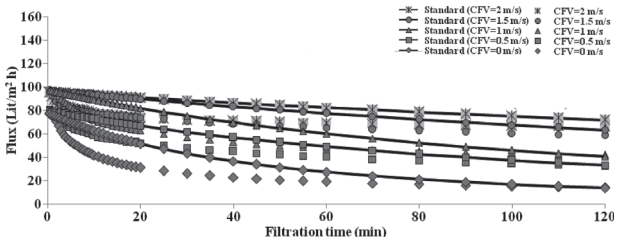

Fig. 10. Permeate flux predicted by the standard pore blocking model at different cross flow velocity with time (pressure 3 bar, oil concentration 1000 ppm and temperature 25 °C).

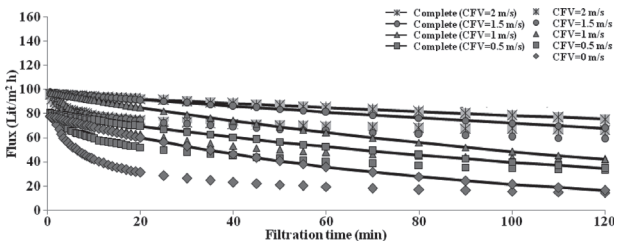

Fig. 11. Permeate flux predicted by the complete pore blocking model at different cross flow velocity with time (pressure 3 bar, oil concentration 1000 ppm, and temperature 25 °C).

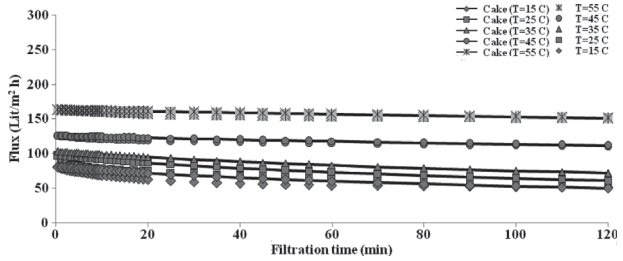

Fig. 12. Permeate flux predicted by the cake layer formation model at different temperature with time (pressure 3 bar, flow rate 1.5 m/s and oil concentration 1000 ppm).

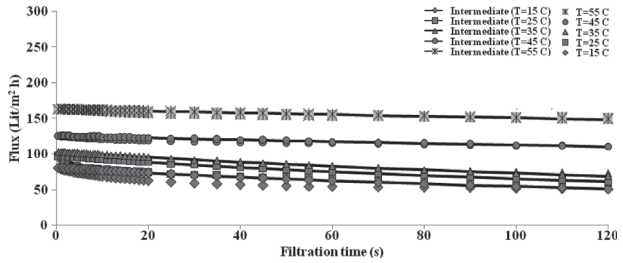

Fig. 13. Permeate flux predicted by the intermediate pore blocking model at different temperature with time (pressure 3 bar, flow rate 1.5 m/s and oil concentration 1000 ppm).

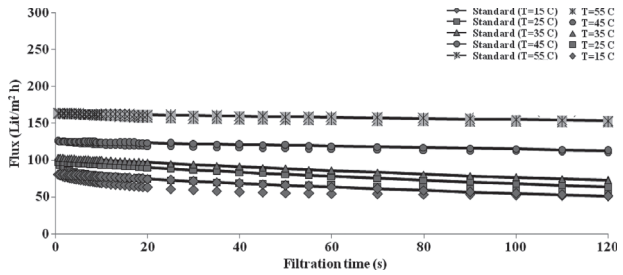

Fig. 14. Permeate flux predicted by the standard pore blocking model at different temperature with time (pressure 3 bar, flow rate 1.5 m/s, oil concentration 1000 ppm).

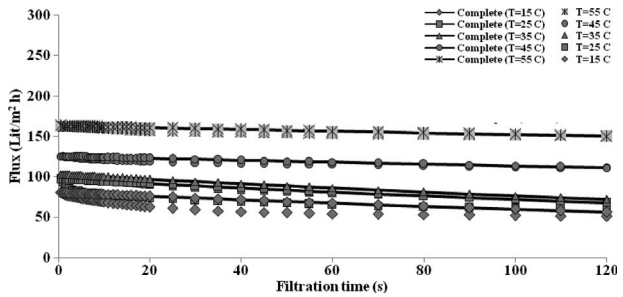

Fig. 15. Permeate flux predicted by the complete pore blocking model at different temperature with time (pressure 3 bar, flow rate 1.5 m/s and oil concentration 1000 ppm).

flux is low and for cake layer formation model, intermediate, standard and complete pore blocking model is 5.9%, 6.55%, 7.5% and 8.45%, respectively.

Figs. 16–19 illustrate that the fitting of the pore blocking mechanisms to the experimental results is good for mullite membrane at different concentration of oil. Lowest deviations between experimental and predicted flux decline were observed in cake filtration model.

The cake layer fouling mechanism occurs when particles/oil droplets are much greater than the membrane pore size. Consequently, they are unable to enter the membrane

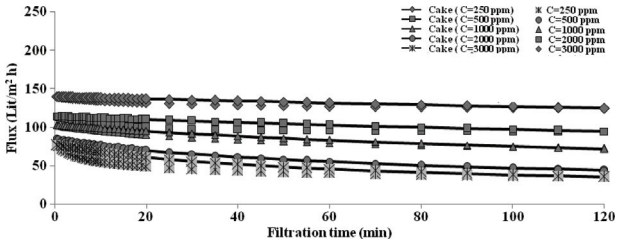

Fig. 16. Permeate flux predicted by the cake layer formation model at different oil concentration with time (pressure 3 bar, flow rate 1.5 m/s and temperature 35 °C).

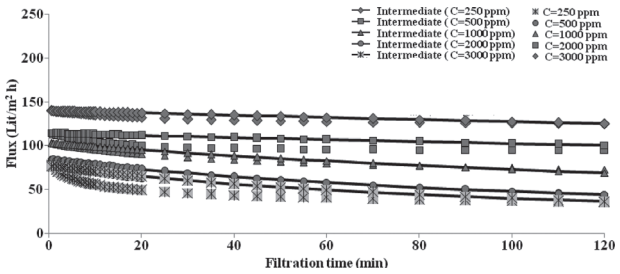

Fig. 17. Permeate flux predicted by the intermediate pore blocking model at different oil concentration with time (pressure 3 bar, flow rate 1.5 m/s and temperature 35 °C).

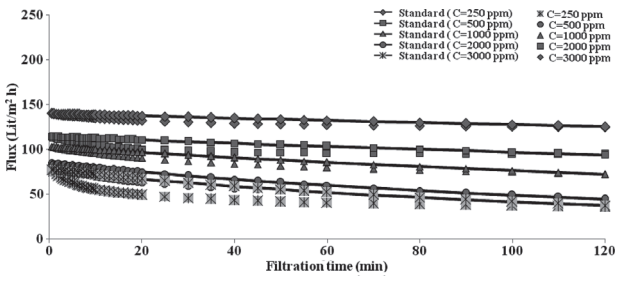

Fig. 18. Permeate flux predicted by the standard pore blocking model at different oil concentration with time (pressure 3 bar, flow rate 1.5 m/s and temperature 35 °C).

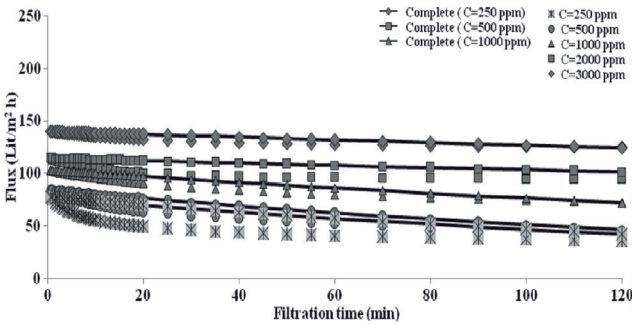

Fig. 19. Permeate flux predicted by complete pore blocking model at different oil concentration with time (pressure 3 bar, flow rate 1.5 m/s and temperature 35 °C).

pores. Some of the main factors that have an influence on the cake layer resistance are: Oil droplets deformation, cake compression and cake layer thickness [15].

Oil droplets deformation may increase the packing density of the cake layer formed and therefore it may favor a higher cake resistance and a lower permeate flux. The denser the cake layer formed is the faster flux decline is obtained. Results show that average percentage error of predicated flux for cake layer formation model, intermediate pore blocking model, standard pore blocking model and complete pore blocking model is 7.64%, 11.83%, 14.75% and 16.70%, respectively.

These experimental results indicate that different filtration mechanisms could be applied simultaneously for the description of the filtration data, which were found during cross flow MF of the present oil-in-water emulsions.

4. Conclusions

One of the treatment techniques used for oil separation from oil-in-water emulsions is membrane filtration. In this work, mechanisms of flux decline of synthetic mullite ceramic microfiltration membranes for treatment of oil-in-water emulsions was investigated. For that purpose Hermia's models were used. Experimental results of permeate flux versus time were compared to the Hermia's fouling models. The best fit to experimental data corresponded mullite ceramic membrane to the cake layer formation model for all the experimental conditions tested. Also, permeate fluxes that predicted by intermediate pore blocking models showed good agreement with the experimental data.

After cake filtration model, the best flux predicted to the experimental data was intermediate pore blocking model and worst predicted flux was for complete pore blocking model.

References

[1] J.J. Kim, Membrane microfiltration of oily water, Macromal. Symp., 118 (1997) 413–418.
[2] J. Mueller, Y. Cen and R.H. Davis, Crossflow microfiltration of oily water, J. Membr. Sci., 129 (1997) 221–235.
[3] J. Marchese, N.A. Ocheoa, C. Pagliero and C. Almandoz, Pilot-scale ultrafiltration of an emulisified oil wastewater, Sci. Technol., 34 (2000) 2990–2996.
[4] B. Chakrabarty, A.K. Ghoshal and M.K. Purkait, Ultrafiltration of stable oil-in-water emulsion by polysulfone membrane, J. Membr. Sci., 325 (2008) 427–437.
[5] P. Srijaroonrat, E. Julien and Y. Aurelle, Unstable secondary oil/water emulsion treatment using ultrafiltration: fouling control by back-ushing, J. Membr. Sci., 159 (1999) 11–20.
[6] J. Kong and K. Li, Oil removal from oil-in-water emulsions using PVDF membranes, Sep. Purif. Technol., 16 (1999) 83–93.
[7] A. Salahi, T. Mohammadi, A. Rahmat pour and F. Rekabdar, Oily wastewater treatment using ultrafiltration, Desal. Water Treat., 6 (2009) 289–298.
[8] W.C. Wong, L.T.Y. Au, C.T. Ariso and K.L. Yeung, Effects of synthesis parameters on the zeolite membrane growth, J. Membr Sci., 191 (2001) 143–163.
[9] S.M. Kumar and S. Roy, Recovery of water from sewage effluents using alumina ceramic microfiltration membranes, Sep. Sci. Technol., 43 (2008) 1034–1064.
[10] J. Hermia, Constant pressure blocking filtration laws-application to power law: Non-Newtonian fluids, Trans. Inst. Chem. Eng., 60 (1982) 183–187.
[11] M. Kazemimoghadam, A. Pak and T. Mohammadi, Dehydration of water/1–1 dimethylhydrazine mixtures by zeolite membranes, Micropor. Mesopor. Mater., 56 (2002) 81–88.
[12] M.C.V. Vela and S. Blanco, Analysis of membrane pore blocking models applied to the ultrafiltration of PEG, Sep. Purif. Technol., 62 (2008) 489–498.
[13] S. Kosvintsev, R.G. Holdich, I.W. Cumming, and V.M. Starov, Modelling of dead-end microfiltration with pore blocking and cake formation, J. Membr. Sci., 208 (2002) 181–192.
[14] K.N. Bourgeous, J.L. Darby and G. Tchobanoglous, Ultrafiltration of wastewater: effects of particles, mode of operation, and backwash effectiveness, Water Res., 35 (2001) 77–90.
[15] S.S. Madaeni, The effect of large particles on microfiltration of small particales, J. Porous Mater., 18 (2001) 143–148.